ECS Transactions, 68 (1) 3535-3551 (2015)
10.1149/06801.3535ecst ©The Electrochemical Society

Understanding of CO_2 Electrochemical Reduction Reaction Process via High Temperature Solid Oxide Electrolysers

X. Yue and J. T. S. Irvine

School of Chemistry, University of St. Andrews, St. Andrews, Fife KY16 9ST, UK

The CO_2 electrochemical reduction via SOEC was studied for a range of cathode materials in various operational conditions. The influences of the fuel gas composition, operating potential and temperature on cathode behavior are discussed and compared on different cathodes. The dissociative adsorption and surface diffusion of active species from CO_2 reduction reaction was found to contribute dominantly to the LSCM-based cathode working in CO_2-CO mixtures. Efforts were also made to obtain a high performance and durable cathode for high temperature CO_2 electrolyser by employing a gradient LSCM-YSZ cathode and by adopting wet impregnation in cathode preparation. The latter was to more effective in enhancing the cathode electro-catalytic activity. A competitive cathode to Ni-YSZ cermet was fabricated by infiltrating 0.5wt% Pd and GDC into porous LSCM and YSZ layers.

Introduction

Solid oxide electrolysis cells (SOECs) consist of a gas tight, ion-conducting electrolyte sandwiched between two porous electrodes; the same type of device can work reversely as solid oxide fuel cells (SOFCs), which have been developed significantly in the recent two decades (1-2). The application of CO_2 electrolysis by SOEC possesses potential rewards both in energy and environmental aspects. It offers a way to recycle CO_2 into chemicals and value-added fuels, which helps to reduce the accumulation of atmospheric CO_2 and realize the carbon neutral cycling of fuels. Compared to H_2 from steam splitting via SOECs, the synthetic fuels from CO_2 electrolysis are compatible with the existing infrastructure for petroleum fuels transportation and storage, which thus saves the necessity and costs for building up a brand-new infrastructure based on H_2 economy (3). Secondly, SOEC techniques provide a means to utilize the intermittent and decentralized renewable sources, such as wind, tide, etc., as energy input to store excess electricity in the form of H_2, CO and hydrocarbons and use these chemicals when necessary.

Compared to low temperature CO_2 electrolysis in liquid system, the high temperature SOECs have some positive characteristics, including lower electric energy requirement, wide range of options for electrode material, and fast electrode kinetics at SOEC operation temperature (600-1000^{o}C) (4). However, it is a challenging task to realize efficient reduction of CO_2 by SOEC due to the non-polar nature of CO_2 fuels which are hard to be chemically absorbed and activated in high temperature range (5). The CO product from CO_2 reduction is also demanding for the choice of fuel electrode (i.e. cathode in SOEC and anode in SOFC) materials and for the engineering of operation

conditions, especially a long-term test, which has been an issue for the CO/hydrocarbon-fuelled SOFCs. To date, the CO_2 electrolysis by SOEC is still at the starting point, and the mechanisms for the electrochemical reduction of CO_2 through SOECs are not fully understood. Extensive efforts need to be dedicated to the material developments, mechanism study, and system designs, etc.

The cathode materials for high temperature CO_2 electrolysis and the corresponding cathode reaction mechanisms are the focus of this study. Previously, we have investigated and compared the CO_2 electrolysis performance on a range of cathode materials, including Ni-yttria stabilized zirconia (YSZ) cermet, $(La_{0.75}Sr_{0.25})_{0.97}(Cr_{0.5}Mn_{0.5})O_{3\pm\delta}$ (LSCM)-YSZ 50-50 (weight ratio hereinafter) composite and LSCM-($Gd_{0.1}Ce_{0.9}O_{1.95}$ (GDC) 50-50 composite (6-7). Results revealed that Ni-YSZ cermet cathode suffered from carbon deposition after testing in various CO_2-CO mixtures though it showed the best performance at 900^{o}C among the materials examined and that the LSCM-GDC composite, compared to LSCM-YSZ composite, was promising in CO_2 electrolysis operation except at open circuit voltage (OCV) where much larger polarization resistance appeared on the LSCM-GDC composite cathode due to high temperature sintering. The screen printing-derived microstructure for LSCM-based cathode was therefore not good enough for high performance CO_2 electrolysis. In terms of cathode mechanism, distinct impedance behavior was observed from these different cathodes and upon varying operational conditions.

Focused on LSCM based cathodes which were found to be carbon-resistive, effort was made in our lab to find a highly performing, long-term durable cathode for electrochemical reduction of CO_2 by SOEC and to obtain more understanding of the mechanism of CO_2 electrochemical reduction process. The microstructure of LSCM-based cathodes was tuned by the strategy of applying a gradient composite cathode and of adopting wet impregnation as cell fabrication procedures. The electrochemical performance of CO_2 electrolysis was characterized in various CO_2-CO mixtures and applied potentials in 900-750^{o}C with the aid of impedance spectroscopy, on YSZ electrolyte supported three-electrode SOECs. In this paper, some results from the preliminary tested Ni-YSZ cermet and screen-printed LSCM based cathode will be reviewed. Impedance behavior of the electrochemical reduction reaction of CO_2 from different cathode SOECs will be correlated with the variations in gas composition, operating temperature and loading potential. Areas of discussion will include as well how the cathode microstructure impacts the impedance behavior and the corresponding elementary steps from CO_2 electrochemical reduction.

Experimental

SOEC Fabrication

The three-electrode single cells that were fabricated in this paper have thick YSZ pellet as electrolyte and identical air/oxygen electrode material, $(La_{0.75}Sr_{0.25})_{0.95}MnO_3$-scandium stabilized zirconia (LSM-ScSZ) 50-50 composite, as so, the focus of our study was on cathode material selection and cathode performance comparison. 2mm thick YSZ pellets were pressed and sintered at 1500^{o}C. The surfaces of the as-sintered pellets were polished before introducing cathode and anode. Different procedures were employed in cathode preparation, which will be described in the following parts. The LSM-ScSZ

anode was screen printed on the counter side of cathode and fired at 1100°C for all single cells preparation. The geometry of the prepared SOECs was shown before in Ref. (8).

TABLE I. Sintering conditions of diverse cathode materials.

Cathode material	Sintering temperature (°C)	Dwelling time (Hour)
NiO-YSZ	1350	1
LSCM-YSZ	1200	2
LSCM-GDC	1200-1300	2
Graded LSCM-YSZ	1200	2

Screen-printing Derived Cathode Preparation. As explained previously (6), this simply involved printing the slurry of pre-mixed cathode components and organic vehicles on the surface of YSZ pellet, and sintering at high temperature to burn off the organics and obtain a percolated cathode and a well-attached interface between electrolyte and cathode. Cathodes prepared in this manner included Ni-YSZ (corresponding to a weight percentage of 65-35 for NiO-YSZ) cermet, LSCM-YSZ (50-50 by mass) composite, LSCM-GDC (50-50 by mass) composite. The sintering temperatures of these cathodes are listed in Table I. As for the LSCM-YSZ gradient cathode, a thin layer of LSCM-YSZ 30-70 was screen-printed on the surface of YSZ pellet, followed by printing a layer of LSCM-YSZ 60-40 on top of the thin layer and firing the co-layers at high temperature.

Wet-impregnation Derived Cathode Preparation. This route of cathode preparation was adopted for LSCM-GDC set of cathode material. The impregnation-derived LSCM-GDC cathode preparation involved introducing GDC nitrates precursor solution into a pre-printed and sintered LSCM porous skeleton. The porous skeleton was formed by adding graphite and glassy carbon pore formers into the solid contents in screen printing slurry preparation. In order to improve the interfacial bonding between cathode and electrolyte, a porous YSZ layer was screen-printed on the surface of YSZ pellet, prior to printing porous LSCM layer on top of that. These two porous layers were co-fired at 1300°C. After this, GDC nitrates solution were infiltrated into the LSCM-YSZ porous backbone, and fired at 500°C to decompose nitrates into oxide. These steps were repeated until a 50-50 weight ratio of GDC to LSCM-YSZ was obtained. The following was sintering the as-prepared cathode at 1100°C and the introduction of LSM-ScSZ anode at the other side of YSZ pellet. A dopant level of Pd extra catalyst was also incorporated into the impregnation derived LSCM-GDC cathode, in which case Pd nitrate solution was infiltrated into the GDC-LSCM -YSZ matrix.

SOEC Performance and Microstructure Characterization

The set-up that was used for electrochemical test was shown before (6). Pt paste designed for current collection was painted to both cathode and anode of the as-prepared SOEC and fired at 850°C. The cell was then mounted and semi-sealed at the fuel chamber to the testing set-up, and heated up in N_2 to 900°C, at which 5% H_2/Ar (in 3% H_2O) was introduced into the fuel chamber. This was to reduce NiO to metallic Ni in the case of Ni-YSZ cermet cathode. Otherwise, N_2 was directly switched to various CO_2-CO mixtures when temperature stabilized at 900°C.

The examined CO_2 concentrations in CO_2-CO mixture were 10, 30 and 50 vol. % for Ni-YSZ cermet which was sensitive to coking, and it was up to 70% for LSCM based

cathode. Electrochemical impedance spectroscopy was recorded in each atmosphere at steady state at open circuit voltage (OCV or Eoc), as well as different loadings, which will be referred to (E-Eoc) (i.e. overpotential) equaled 0.2, 0.5, 1.0V respectively throughout this paper. The frequency for impedance measurement ranged from 10^5 to 0.1 or 0.015Hz, with an amplitude of 10mV. After completing the measurement at 900°C, the cell was cooled stepwise to 850, 800, and 750°C in CO_2-CO 70-30 mixture, and impedance spectra were measured at each of these temperatures as at 900°C.

Upon finishing electrochemical test, the cell was cooled down to room temperature, at which it was retrieved for post-mortem characterizations. The microstructure of different cathodes after electrochemical test was inspected by scanning electron microscopy (SEM) and the equipment used were Jeol JSM 5600 (with tungsten filament) and Jeol JSM-6700F (with field emission gun). The energy-dispersive X-ray spectroscopy (EDX) was incorporated with SEM for element identification, and an Oxford INCA Energy 200 device was coupled with SEM instrument for this purpose.

Results

Ni-YSZ Cathode

Figure 1 shows the impedance spectra from Ni-YSZ cermet cathode working in a range of CO_2-CO mixtures at OCV at 900°C. The microstructure and more detailed results of Ni-YSZ cermet as SOEC cathode were reported in ref (6). Clearly, there are two well separated arcs on the impedance spectra of Ni-YSZ cermet cathode in various CO_2-CO systems, with a characteristic frequency at high frequency range increasing with CO concentration. The magnitude of the high frequency arc seems not to change much with varying CO_2/CO concentrations. However, the low frequency arc decreases significantly with increasing CO content in feed, with a characteristic frequency around 0.1Hz (not labeled in Figure 1). Similar trends were found from the impedance spectra of the same cathode working at different potentials in a fixed ratio of CO_2/CO mixture (6).

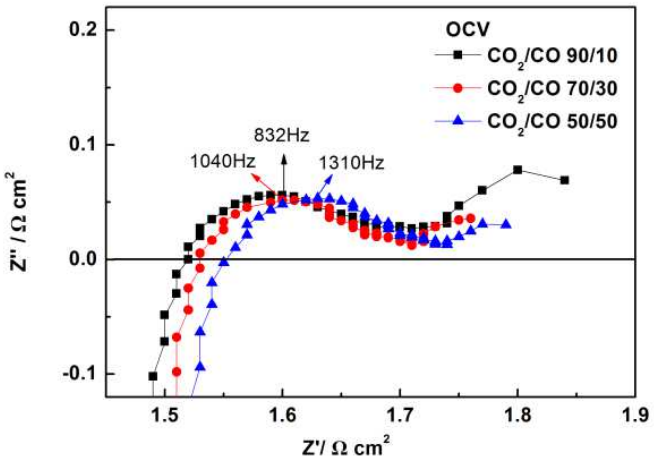

Figure 1. Impedance spectra of Ni-YSZ cermet cathode operating in a series of CO_2-CO mixtures at OCV at 900°C: square indicates CO_2/CO 90/10 mixture, with circle CO_2/CO 70/30 and triangle CO_2/CO 50/50; the characteristic frequency at which a highest imaginary part appears for a arc is revealed (the impedance spectra were recorded from 10^5 to 0.1Hz at an amplitude of 10mV).

In an impedance spectrum, the intercept of the impedance arc with real axis at high frequency end stands for the series resistance (Rs), i.e., ohmic resistance of the tested specimen, while the difference between the intercepts of impedance arc with real axis at high frequency end and low frequency end reflects the polarization resistance (Rp). In Figure 1, the Rs increases while Rp decreases slightly with increasing CO concentration in fuel gas. In a certain atmosphere, for instance, CO_2-CO 70-30 mixture, it was found that the Rs kept constant whereas Rp decreased with increasing potential, with the decrease mainly from the low frequency Rp.

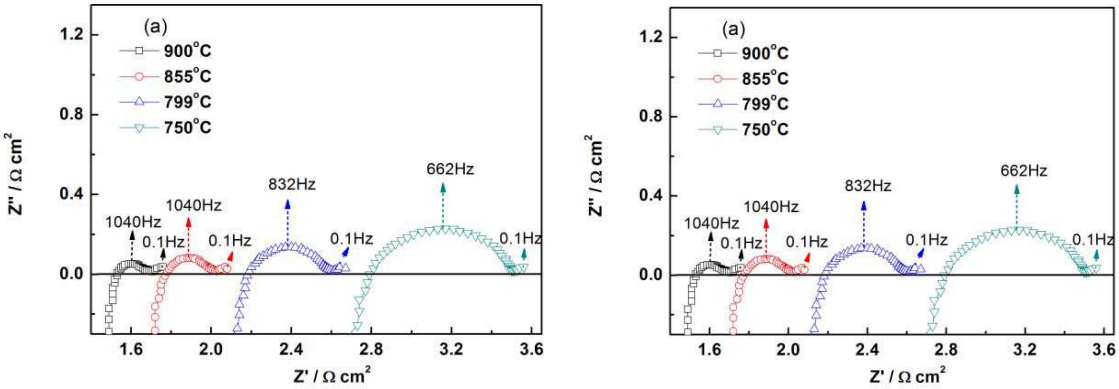

Figure 2. Impedance spectra from Ni-YSZ SOEC cathode operating at OCV (a) as well as at (E-Eoc) of 1.0V (b) in the temperature range of 900-750°C in CO_2-CO 70-30 mixture (the characteristic frequency for the corresponding arcs are labeled).

Figure 2 exhibits the comparisons of impedance spectra from Ni-YSZ cermet cathode working at different potentials at CO_2-CO 70-30 atmosphere in the temperature range of 900-750°C at an interval of ca. 50°C in a cooling operation. As operation temperature drops, both Rs and Rp increase considerably, thereby the cathode performance declines significantly. In addition, the Rs value drops slightly at a loading of 1.0V, in comparison with Rs at OCV, especially at a temperature as low as 750°C, whereas Rp increases evidently when working at high voltage, probably as a consequence of carbon deposition on Ni-YSZ cathode. Carbon was detected ex-site by SEM-EDX on Ni-YSZ cermet cathode after SOEC operation in various conditions.

Noticeably in Figure 2, the high frequency arc increases a lot with lowering operating temperature, with its summit frequency decreasing with temperature, while this characteristic frequency seems potential independent. With respect to the low frequency arc, it does not change much with varying temperature at OCV, and with decreasing temperature it appears to be a tail following the high frequency arc. However, it developed to a small arc upon applying cathodic potential, making its Rp larger than at OCV, and this is very observable at low temperature, such as 750°C in Figure 2(b).

LSCM-YSZ Composite Cathode and Gradient LSCM-YSZ Cathode

Figure 3 displays the impedance spectra of LSCM-YSZ composite cathode working in various CO_2-CO systems at OCV at 900°C (Figure 3(a)) and in a fixed ratio of CO_2/CO mixture at different potentials at 900°C (Figure 3(b)). The polarization curves of the SOEC with this cathode in the same conditions were reported previously. In Figure 3, it can be observed that at least three overlapped arcs present in the impedance spectra of

LSCM/YSZ composite cathode in the testing conditions, a small depressed arc at the high frequency range followed by a large one at the middle frequency zone, and a small arc (a tail when the frequency range is 10^5-0.1Hz) at the low frequency end. The impedance responses from the LSCM-YSZ composite cathode are quite different from what we have seen from Ni-YSZ cermet cathode measured in the same conditions.

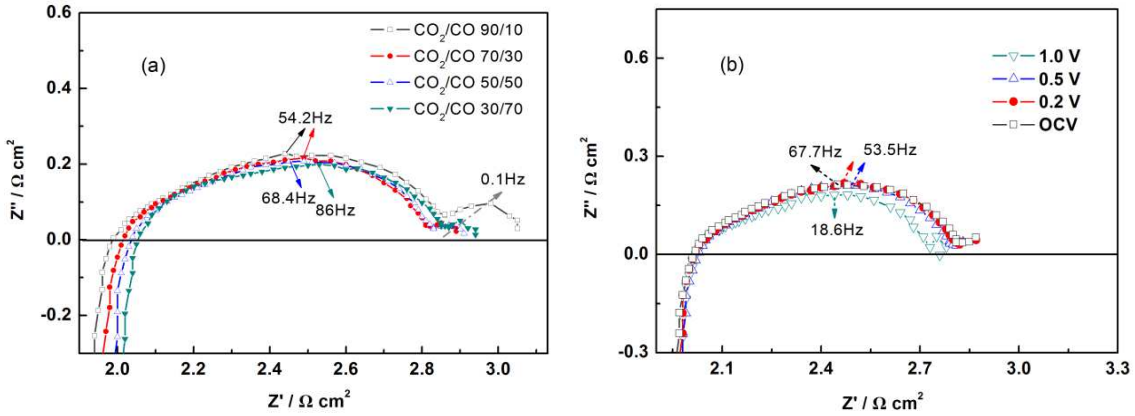

Figure 3. Impedance spectra of LSCM-YSZ composite cathode operating (a) in different CO_2/CO mixtures at OCV at 900°C (frequency range: 10^5 - 0.015Hz) and (b) in CO_2/CO 70/30 mixture at different potentials at 900°C (frequency range: 10^5 - 0.1Hz).

In Figure 3(a), it is impossible to separate the high frequency arc from the intermediate frequency arc, as only one characteristic frequency is found from the complex impedance spectra; therefore, they will be mentioned as high frequency responses compared to the low frequency arc. With increasing CO content in feed gas, the high frequency responses show a slightly increasing characteristic frequency, with a constant characteristic frequency for the arc at the far right of the complex impedance spectra. Additionally, the magnitude of the high frequency responses does not change much with varying CO_2/CO concentration, whereas the magnitude for the low frequency arc decreases evidently when CO_2 ratio in feed gas declines.

In Figure 3(b), the high frequency responses from LSCM-YSZ composite cathode tested in a fixed ratio of CO_2/CO mixture do not change much with varying operating potential neither, they decrease slightly only at a very high loading (1.0V), and the characteristic frequency for the high frequency responses decreases with increasing loading. The Rp values from the LSCM-YSZ composite cathode in the above mentioned testing conditions are around 1.0 Ωcm^2, which are doubled compared to the Rp values from Ni-YSZ cermet under the identical conditions, indicating insufficient activity of LSCM/YSZ towards CO_2 reduction though optimizations could to be done for cathode performance improvement.

The impedance spectra of the LSCM-YSZ composite cathode working in CO_2-CO 70-30 mixture at different temperatures at OCV as well as at 1.0V are displayed in Figure 4. It is interesting that at OCV, the intermediate frequency arc gradually stands out when temperature drops, and the small tail at the extremely low frequency end observed at high temperature becomes invisible at lowered temperatures, probably overlapped with the intermediate frequency arc. At 1.0V loading, the cathode performance is greatly enhanced compared to that in OCV condition, and this tendency becomes significant as

temperature drops, with both Rp and the magnitude of impedance arcs decrease remarkably. At 750°C, the Rp value at 1.0V is as small as half of the value at OCV. Further, only one arc is observed at 1.0V at 750°C with its characteristic frequency at 85Hz, much higher than that was found at OCV, indicating the overlapping of the impedance arcs at high frequency and low frequency. Similar trends are seen at other temperatures except at 900°C.

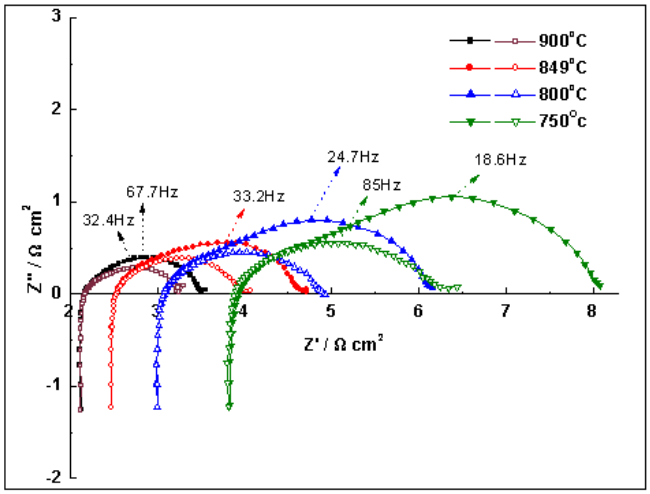

Figure 4. Impedance spectra of LSCM/YSZ cathode working at OCV (solid symbols) and at (E-Eoc) =1.0 V (open symbols) in CO_2/CO 70/30 atmosphere at different temperatures in the range of 900-750°C (frequency ranges from 10^5 down to 0.1Hz).

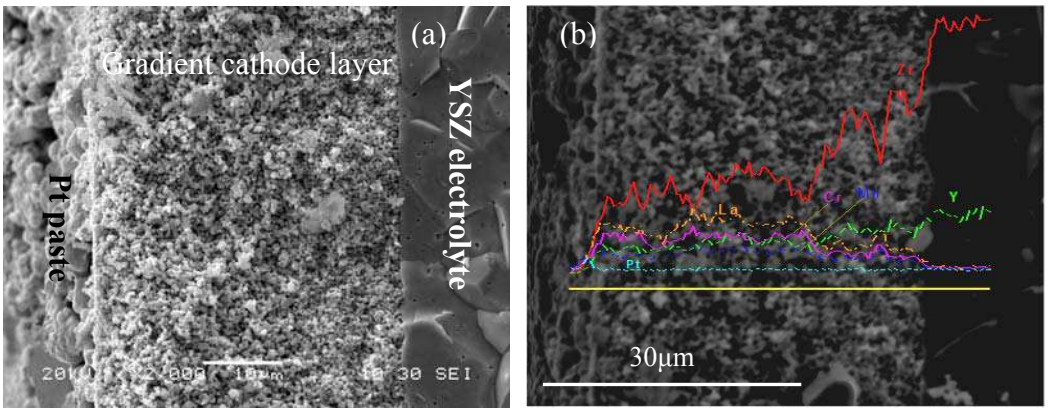

Figure 5. SEM micrograph (a) and the SEM-EDX result (b) of the graded LSCM-YSZ cathode and cathode/electrolyte interface after operation in CO_2-CO mixtures at 900°C.

Effort was made to improve the cathode activity of LSCM-YSZ composite by adopting a gradient cathode which consists of a relatively thin LSCM-YSZ 30-70 layer adjacent to the dense YSZ electrolyte and a layer of LSCM-YSZ 60-40 at the outer side of cathode. The gradient cathode was prepared in a similar manner as the LSCM-YSZ composite cathode that is composed of a single layer of LSCM-YSZ 50-50. The SEM microstructure of the gradient cathode after testing in CO_2-CO mixtures at 900°C is illustrated in Figure 5(a). From the SEM cross-sectional view, the LSCM-YSZ gradient cathode consists of two layers, the inner LSCM-YSZ 30-70 layer that is close to the electrolyte and the outer LSCM-YSZ 60-40 layer. The thickness of the inner and outer cathode layer is ca. 15 and 25μm, respectively, which has been confirmed by SEM-EDX

line-scan results showed in Figure 5(b). As expected, graded distributions of elements in LSCM and YSZ phases are clearly seen in Figure 5(b). The gradient cathode also contacts very well with the dense electrolyte.

The electrochemical results from the gradient LSCM-YSZ cathode for high temperature CO_2 electrolyser are shown in Figure 6, in which the impedance spectra from the gradient cathode and the normal LSCM-YSZ cathode are compared with different level of loads being applied to both cathodes in CO_2-CO 70-30 system at 900°C. The Rs was corrected as Rs mainly came from the ca. 2 mm thick YSZ electrolyte; therefore, Rs from lateral electrodes were neglected for both cathode cells.

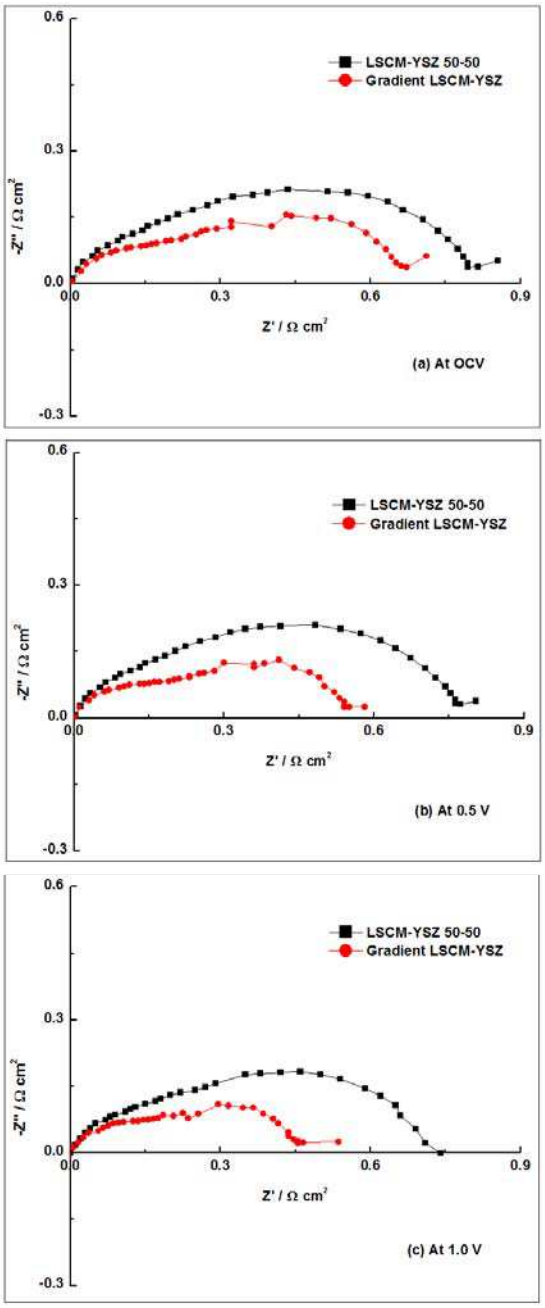

Figure 6. Performance comparisons of LSCM-YSZ 50-50 composite cathode (square symbols) and the graded LSCM-YSZ cathode (circle symbols) working at OCV (a), 0.5V (b) and 1.0V (c) in CO_2/CO 70/30 mixture at 900°C.

It can be observed in Figure 6 that the Rp from the graded LSCM-YSZ cathode is smaller than that from the averaged composite cathode under OCV condition, and with the gradient cathode components, the impedance arcs are distinctly suppressed, implying that the graded structure is advantageous for improving cathode performance. The above phenomena get more pronounced in electrolysis operation conditions, e.g. at 0.5V and at 1.0V in Figure 6 (b) and (c). At 1.0V, the Rp values are 0.47 and 0.74 Ω cm^2, respectively for the gradient and normal LSCM-YSZ cathodes. Noting that the shape and outline of the impedance arcs are hardly changed, though the size of impedance arcs from the gradient cathode are remarkably reduced, which may be indicative that the rate limiting processes for cathode reaction, i.e. the CO_2 electrochemical reduction, are consistent for the gradient cathode and the one with average LSCM-YSZ composite.

Screen-printed LSCM-GDC Composite Cathode

LSCM-GDC composite cathode was prepared similar to LSCM-YSZ composite cathode, but fired at 1300°C, which was essential to obtain a good interfacial bonding of cathode to electrolyte. The GDC component was believed to be favorable over YSZ as it has higher ionic conductivity and most importantly, it has excellent catalytic properties towards a series of oxidation and reduction reaction. Figure 7 displays the impedance spectra of the screen-printed LSCM-GDC composite cathode working in a range of CO_2-CO mixtures at OCV at 900°C. More electrochemical results from this cathode were covered in Ref (6).

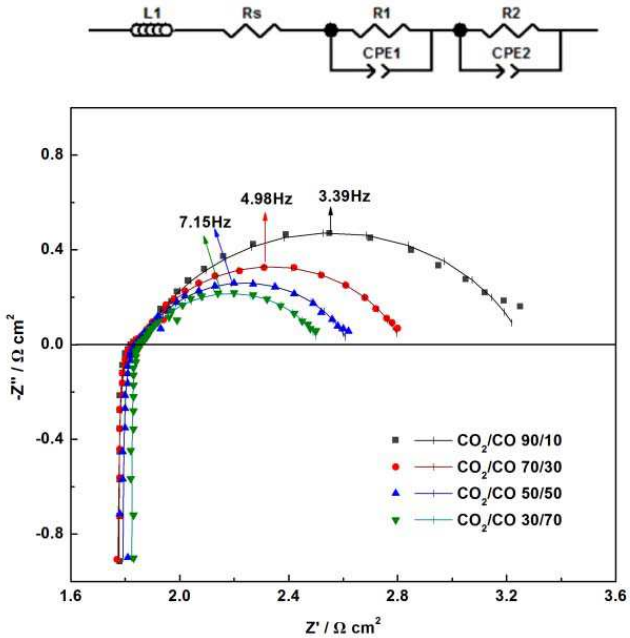

Figure 7. Impedance spectra of the cell with LSCM/GDC cathode operating in different atmospheres at OCV at 900°C (solid symbols) together with fitted results (straight lines) (the equivalent circuit used to fit the experimental data is on top of impedance spectra).

In Figure 7, a distinct Gerischer-type of impedance dispersion, which is a linear response at high frequency range followed by a semi-circle at low frequency region, is observed on screen-printed LSCM-GDC cathode in various CO_2-CO systems at 900°C. The characteristic frequency for the low frequency semi-circle increases slightly with increasing CO concentration in fuel gas, and the low frequency arc becomes smaller with

the same variation in fuel gas. Similar impedance dispersions were also seen on this cathode working at different levels of loads (6-7). The impedance data are well fitted using the equivalent circuit shown on top of impedance spectra in Figure 7.

The impedance spectra of LSCM-GDC composite cathode working at OCV at different temperatures from 900-750°C are reveal in Figure 8. It is noticed that the linear dispersion at high frequency zone evolves to a small arc on LSCM-GDC composite cathode when operation temperature drops from 850 to 750°C, distorting it from the Gerischer impedance observed at 900°C. As temperature decreases, the high frequency arc is characterized at 527Hz, which is independent of operation temperature, whereas the low frequency arc is featured at 4.98, 2.24, 1.43, and 0.89Hz at 900, 850, 800, and 750°C respectively.

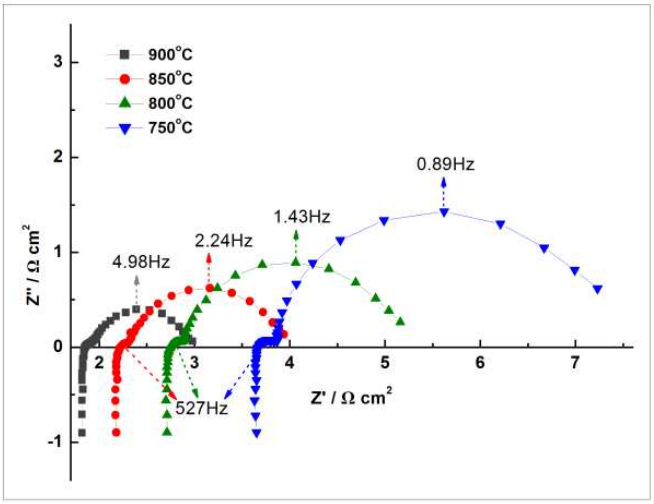

Figure 8. Impedance spectra of LSCM-GDC composite cathode being cooled from 900°C to 750°C at an interval of 50°C at OCV at CO_2-CO 70-30 atmosphere.

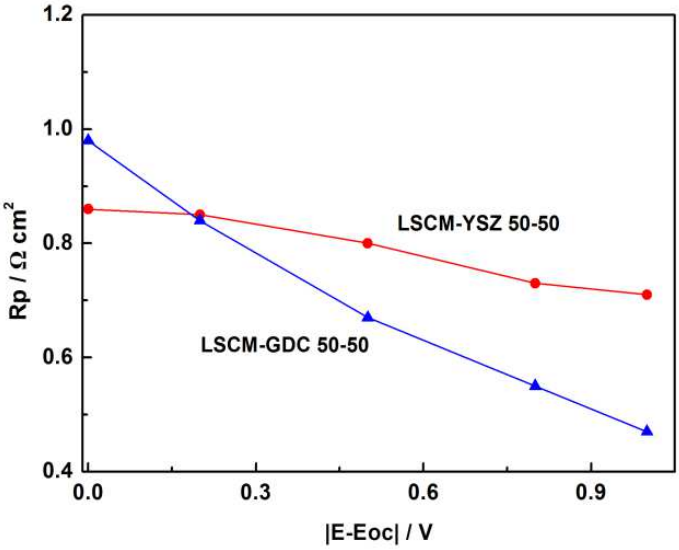

Figure 9. Comparison of Rp values from LSCM-YSZ composite and LSCM-GDC composite cathode operating in CO_2-CO 70-30 mixture at different potentials at 900°C.

The cathode performance towards CO_2 electrolysis via SOEC is compared between LSCM-YSZ composite and LSCM-GDC composite, with their Rp in CO_2-CO 70-30

mixture at different potentials at 900°C shown in Figure 9. At OCV, it is apparent that the LSCM-YSZ composite performs better than LSCM-GDC analogue working in the same conditions, nevertheless, the latter starts to excel the former at (E-Eoc) higher than 0.2V, with the Rp values from LSCM-GDC cathode dropping significantly while those from LSCM-YSZ cathode not changing much with increasing potential.

Figure 10 exhibits the cathode resistances at OCV from LSCM/YSZ composite (Figure 10(a)) and LSCM/GDC composite (Figure 10(b)) as a function of the reciprocal temperature, i.e., the Arrhenius plots in CO_2/CO 70/30 atmosphere. It can be seen that the Arrhenius plots show good linearity over the whole temperature range and the linear fit presents activation energy of ~55-58 kJ mol^{-1} for area specific resistance (ASR, the sum of Rs and Rp) from LSCM based cathode, much smaller than the value (~100 kJ mol^{-1}) obtained from pure $Gd_{0.4}Ce_{0.6}O_{2-\delta}$ cathode in similar CO_2-CO atmosphere (9).

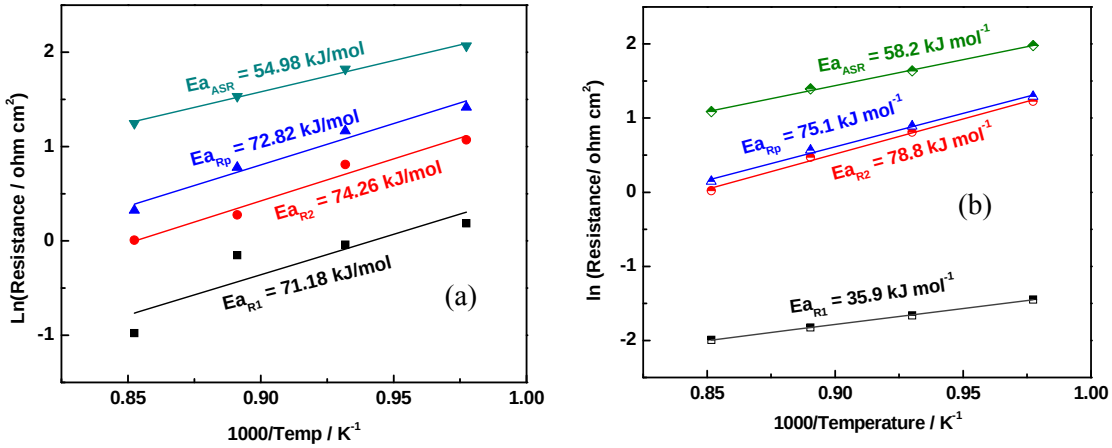

Figure 10. Arrhenius plots of the resistance from (a) LSCM-YSZ and (b) LSCM-GDC composite cathode at OCV as a function of operation temperature (R1 and R2, values obtained by impedance fitting using the equivalent circuit displayed in Figure 7, stands for polarization resistances corresponding to high frequency and low frequency arc from both cathode respectively, with Rp as a sum of R1 and R2).

Further, the Arrhenius plots provide activation energy of ca. 73, 71, and 74kJ mol^{-1} for Rp, R1, and R2 respectively for LSCM/YSZ cathode. With respect to LSCM/GDC composite cathode, the Arrhenius plots give activation energy of ca. 75, 36, and 79kJ mol^{-1} for Rp, R1, and R2, respectively. Apparently, both the activation energy of R1 and R2 are close to that of Rp for LSCM/YSZ composite, whilst the activation energy of R1 is much lower than that of Rp, with activation energy of R2 close to Rp, for LSCM/GDC cathode.

Impregnation-derived LSCM-GDC Cathode

It has been shown in previous section that a graded cathode microstructure is beneficial for enhancing cathode electro-catalytic activity; however, this was not applied to LSCM-GDC composite cathode, due to the concerns of possible solid phase reaction between the two components and of increasing interfacial resistance upon increasing GDC content in the layer close to YSZ electrolyte (10,11). Instead, a LSCM-GDC cathode derived from wet impregnation was fabricated which was detailed in section 2.1. The microstructure of this cathode can be found in details in Ref (12).

Figure 11(a) presents the performance from the GDC impregnated LSCM-YSZ cathode tested in OCV condition in CO_2-CO mixtures at 900°C. Compared to screen-printed LSCM-GDC composite, the infiltration induced LSCM-GDC cathode exhibits remarkably small impedance arcs, one locating at a summit frequency of 527Hz which is independent of atmosphere and another one positioning at a characteristic frequency of around 1Hz. The Rp from the impregnated cathode is a few times smaller in comparison with the screen-printed LSCM-GDC analogue in the identical conditions, suggesting the outstanding electro-catalytic properties in LSCM-GDC cathode brought by wet impregnation. In addition, the cathode performance is further boosted with the introduction of 0.5wt% Pd catalyst into impregnation-derived GDC-LSCM-YSZ matrix, as illustrated in Figure 11(b). Even smaller Rp values are observed from the GDC impregnated LSCM-YSZ cathode with the aid of a small amount of Pd extra catalyst. Only one discernible and markedly depressed arc is presented in the impedance spectra in Figure 11(b), except in the fuel with very large amount of CO_2 which seems to have an extra arc at extremely low frequency.

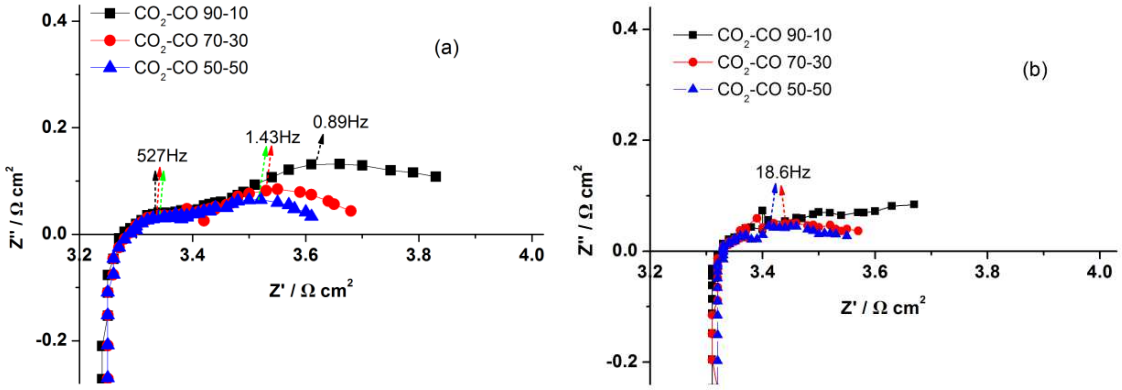

Figure 11. Impedance spectra from the impregnation-derived LSCM-GDC SOEC cathode measured in different CO_2-CO mixtures at OCV at 900°C (a) bare LSCM-GDC cathode (b) GDC impregnated LSCM cathode with 0.5wt% Pd.

The temperature-dependent impedance from the GDC infiltrated LSCM-YSZ cathode with and without Pd catalyst were also measured (not shown here). From the bare GDC impregnated LSCM-YSZ cathode, two separated impedance arcs were found at all operation temperatures, with the high frequency arc locating at a constant characteristic frequency (527Hz) in the measured temperature range while the low frequency arc varying significantly with temperature. Both arcs increased in magnitude with the low frequency arc changing more obviously. These are similar to the phenomena observed from the screen-printed LSCM-GDC cathode working in identical conditions. As for the Pd-GDC co-impregnated LSCM-YSZ cathode, similar trends were observed for the low frequency responses in impedance spectra, however, the responses in the high frequency range seemed to be linear in the complex impedance spectra, which make it hard to separate the arcs as seen from the cathode without Pd catalyst.

Discussion

In previous section, the cathode performance towards high temperature CO_2 dissociation via SOEC was characterized in a scope of materials, including Ni-YSZ cermet, LSCM-YSZ composite and LSCM-GDC composite prepared in different

procedures, by impedance spectroscopy. The impedance spectra from different cathodes were compared in various operation conditions. Factors including fuel composition, potential and working temperature were considered.

Ni has excellent electric and intrinsic catalytic properties towards CO oxidation/CO_2 reduction reaction, indicated by the much smaller Rp values from Ni-YSZ cermets cathode compared to screen-printed LSCM-YSZ and LSCM-GDC composite cathode. On the other hand, it also has good catalytic properties for C-C/C-H bond breaking which leads to coke formation (13,14). The increase in Rs value with increasing CO concentration observed from Ni-YSZ cermet cathode (Figure 1) is probably due to the coke formation from Boudouard reaction. Although carbon formation by Boudouard reaction is not thermodynamically favorable at such a high temperature as 900^{o}C, it is impossible to eliminate its occurrence as a result of local CO-rich condition. The carbon deposition can be confirmed by the enlargement in Rp with increasing potential at 750^{o}C, which is hardly seen on other kinds of cathode in similar conditions (Figures 3, 6, and 9).

Concerning the electrochemical CO_2 reduction process happening on Ni-YSZ cermet cathode, it was generally assumed that the high frequency arc indicated the impedance from charge transfer process for CO_2 electrochemical reduction whilst the low frequency arc suggested the impedance from mass transfer processes (6,15,16). However, it has been found that both the high frequency and low frequency arcs are dependent on fuel composition, potential as well as temperature, which reflects that it is difficult to clarify the contributions of charge transfer and mass transfer processes to either the high frequency arc or the low frequency arc, in other words, the observed response might be overlapped arcs with close relaxation times. With the occurrence of carbon deposition, it is more complicated to explain the electrochemical processes taking place on Ni-based cathode, though the low frequency arc seems to be affected more by carbon formation.

On the cathodes that are composed of fully oxides, very different impedance responses are detected (Figures 3-4 and 6-8). On LSCM-YSZ composite cathode, the high frequency related processes are less dominant compared to the intermediate frequency processes. The mixed electronic and ionic conductivity in LSCM, especially in reducing atmosphere, is probably beneficial for the high frequency process including charge transfer (8). However, the insufficient electro-catalytic activity from LSCM also makes the Rp 2-4 times larger than Rp from Ni-YSZ cermet cathode in the same conditions (Table II). On LSCM-YSZ cathode (Figures 3 and 4), when temperature is lowered, the small tail-shaped arc at extremely low frequency becomes overlapped with the one following the high frequency arc at OCV, with the low frequency arc being affected more profoundly with varying temperature. This is apparently different from what has been observed on Ni-YSZ cermet cathode. At 750^{o}C, the high frequency impedance situated at 662Hz dominates the cathode performance from Ni-YSZ cermet, nonetheless, the impedance positioning at a characteristic frequency of 18.6Hz is more responsible for the LSCM-YSZ cathode performance. In fact, the low frequency arc sitting at a summit frequency in the range of 19-0.1Hz, likely to be the surface kinetics in cathode reaction, is found to be the limiting factor for the LSCM-based cathode in high temperature CO_2 electrolyser (Figures 4, 8 and 11). At a loading of 1.0V to LSCM-YSZ cathode at different temperatures, the low frequency arc reduces tremendously compared to that at OCV, the high frequency arc however stays the same as that at OCV, which

means that the surface activity of LSCM-YSZ composite is greatly boosted by applying external loads, especially at lowered temperatures.

The introduction of a gradient LSCM-YSZ composite improves the LSCM-YSZ cathode performance towards CO_2 dissociation via SOEC. In this composite, LSCM is the catalyst and YSZ provided most oxide ion conducting paths. Compared to LSCM/YSZ 50/50 composite cathode, the higher content of YSZ component in the layer adjacent to electrolyte and LSCM-rich component in the cathode outer layer are possibly advantageous for the processes happening in these regions, likely the charge transfer and dissociated oxide ion diffusion processes in the inner layer and surface reactions at the outer cathode. According to literature review, gradient composite would introduce gradient distribution of particle sizes, pores and concentrations, which are believed to be beneficial for expanding TPB area and mass transfer (17,18). As a result, the raised amount of YSZ phase in the inner layer and of LSCM component in the outer layer might lead to enlarged TPB area and thus promoted cathode performance for LSCM-YSZ cathode. Besides, the high level of YSZ phase in the inner layer is helpful for improving cathode/electrolyte contacting, thereby, the cathode/electrolyte interfacial resistance in the gradient structure is probably decreased. Combined with the electrochemical results in Figure 6, it is believed that the graded structure provides more active sites and conducting paths for the cathode reaction, which interprets the higher performance of the gradient LSCM-YSZ cathode over the LSCM-YSZ 50-50 composite cathode.

On the screen-printed LSCM-GDC composite cathode, the Gerischer-type impedance was found in various loadings and CO_2-CO mixtures at 900^oC (Figure 7) (7). This type of impedance indicates a fast charge transfer process followed by a dominant mass transfer processes for CO_2 electrochemical reduction reaction, including dissociative adsorption and the subsequent surface diffusion of the reaction intermediate species to the triple phase boundaries (TPBs), where the electrochemical reactions take place. With temperature dropped, the Gerischer impedance on screen printed LSCM-GDC composite cathode evolves into two well-separated arcs with the low frequency arc significantly larger than the high frequency arc. In 900-750^oC, the high frequency arc grows slightly with a constant summit frequency, whereas the low frequency arc expands greatly with a declining characteristic frequency upon reducing temperature. Therefore, the adsorption/desorption and surface diffusion processes impact the electrochemical reduction of CO_2 predominantly. The same phenomena are observed from the impregnation-induced LSCM-GDC cathode working in different temperatures though the cathode activity is markedly promoted by adopting the wet impregnation.

Regarding the difference of cathode performance between LSCM-YSZ and LSCM-GDC composite from screen-printing, it is of interest to find that the former performs better at OCV and worse at higher potentials than the latter (Figure 9), which means that the LSCM-GDC composite is a promising material for high temperature CO_2 electrolysis. The poor performance from LSCM-GDC composite cathode at OCV was from the sintering of the cathode components during high temperature fabrication and the enhanced cathode activity under operation conditions was believed mainly from the improved properties from GDC component in reducing atmospheres, as discussed before (6). With respect to Arrhenius plots for both cathodes, it is reasonable to see that the activation energy from the high frequency and the low frequency impedances are close to that from Rp on LSCM-YSZ composite and that the activation energy from the high

frequency impedance is much smaller while that from the low frequency impedance is close to the activation energy from Rp on LSCM-GDC composite (Figure 10). This confirms that the low frequency arc contributes dominantly to the performance of LSCM-GDC composite cathode whereas both high frequency and low frequency processes are the limiting steps on LSCM-YSZ composite cathode for CO_2 reduction by SOEC.

TABLE II. Comparison of Rp values from different cathodes operating at OCV at 900°C in various CO_2-CO mixtures.

	Rp values from different cathode (Ω cm^2)				
CO_2-CO ratio	**Ni-YSZ cermet**	**LSCM-YSZ composite**	**Graded LSCM-YSZ composite**	**Screen-printed LSCM-GDC composite**	**Impregnated-derived LSCM-GDC cathode**
90-10	0.33	1.07	0.98	1.49	0.65
70-30	0.23	0.87	0.71	1.05	0.42
50-50	0.24	0.87	0.59	084	0.35

In Table II, the Rp values from different cathodes operating in a range of CO_2-CO mixtures at OCV at 900°C are summarized. It is found that the most effective way to improve the cathode performance for high temperature CO_2 electrolysis is to prepare the LSCM-GDC cathode from wet impregnation, by which the cathode components are introduced and fired separately so that the sintering temperature can be tuned for each component. The Rp values from the GDC impregnated LSCM-YSZ cathode are two times smaller than the screen-printed LSCM-GDC cathode, originating from the extended TPBs from the infiltration-derived cathode microstructure which has the fine GDC particles highly dispersed on the surface of LSCM and YSZ porous layer (12). With introducing 0.5wt% Pd into the impregnation-derived LSCM-GDC cathode, the cathode performance is comparable to Ni-YSZ cermet cathode working in similar conditions (Figure 11(b)).

Conclusions

In this paper, different kinds of cathode materials were applied in high temperature CO_2 electrolyser, and effort was to find a highly performed, long-term durable cathode material for electrochemical reduction of CO_2 by SOEC and to obtain more understandings of the mechanism of CO_2 electrochemical reduction process. The electrochemical performance of CO_2 electrolysis was characterized in various CO_2-CO mixtures and applied potentials in 900-750°C with the aid of impedance spectroscopy, on YSZ electrolyte supported three-electrode SOECs. The impedance behavior of the electrochemical reduction reaction of CO_2 from different cathode SOECs was correlated with the variations in gas composition, operating temperature and loading potential.

The impedance response for CO_2 electrochemical reduction varied with the scope of cathode materials under investigation and the cathode operation conditions, including fuel composition, working potential and temperature. Focus was casted on LSCM-based cathode fabricated via different procedures, although the Ni-YSZ cermet displayed different impedance behavior which was helpful to get a better understanding of the electrochemical processed from CO_2 reduction by SOECs. Two impedance arcs were generally observed on the LSCM-based cathodes, with the low frequency arc positioning at a characteristic frequency in the range of 0.1-18.6Hz depending on the cathode

microstructure and operational conditions. The low frequency arc, likely to be associated with CO_2/CO adsorption/desorption and subsequent surface diffusion of the reaction intermediate species to the active sites, impacted the LSCM-GDC cathode performance dominantly. The CO_2 reduction mechanisms did not vary significantly on the same cathode material while manufactured in different ways, though the cathode performance was distinctly affected by fabrication procedures.

By introducing a LSCM-YSZ 30-70/LSCM-YSZ 60-40 graded cathode, the cathode performance was greatly improved, and the surface activity was profoundly accelerated. However, a more effective way to promote cathode performance was to introduce the cathode components in separate steps via wet impregnation. A competitive CO_2 electrolysis performance to Ni-YSZ cermet was obtained from the GDC impregnated LSCM-YSZ cathode with 0.5% Pd extra catalyst, which also showed a comparable performance between SOEC and SOFC when operating in CO_2-CO 50-50 mixture.

Acknowledgments

The authors thank the University of St Andrews and RCUK Energy Supergen programme on H-Delivery and EPSRC Platform and Senior fellowship programs for funding.

References

1. C. Sun, U. Stimming, *J. Power Sources*, **171**, 247 (2007).
2. A. Kirubakaran, S. Jain, R. K. Nema, *Renew. Sust. Energy Rev.*, **13**, 2430 (2009).
3. Z. Zhan, W. Kobsiriphat, J. R. Wilson, M. Pillai, I. Kim, and S. A. Barnett, *Energy Fuels*, **23**, 3089 (2009).
4. A. Hauch, S. D. Ebbesen, S. H. Jensen and M. Mogensen, *J. Mater. Chem.*, **18**, 2331 (2008).
5. W. Qi, Y. Gan, D. Yin, Z. Li, G. Wu, K. Xie, and Y. Wu, *J. Mater. Chem. A*, **2**, 6904 (2014).
6. X. Yue and J. T. S. Irvine, *J. Electrochem. Soc.*, **159**, F442 (2012).
7. X. Yue and J. T. S. Irvine, *Electrochem. Solid-State Lett.*, **15** (3), B31 (2012).
8. S. Tao and J. T. S. Irvine, *J. Electrochem. Soc.*, **151** (2), A252 (2004).
9. R. D. Green, C. Liu, S. B. Adler, *Solid State Ionics*, **179**, 647 (2008).
10. K. Eguchi, N. Akasaka, H. Mitsuyasu, Y. Nonaka, *Solid State Ionics*, **135**, 589 (2000).
11. A. Tsoga, A. Gupta, A. Naoumidis and P. Nikolopoulos, *Acta Mater.*, **48**, 4709 (2000).
12. X. Yue and J. T. S. Irvine, Modification of the LSCM-GDC cathode to enhance performance for high temperature CO_2 electrolysis via solid oxide electrolysis cell (SOEC), In preparation.
13. P. Holtappels, L. G. J. De Haart, U. Stimming, I. C. Vinke and M. Mogensen, *J. Appl. Electrochem.*, **29**, 561 (1999).
14. J. B. Goodenough, Y. Huang, *J. Power Sources*, **173**, 1 (2007).
15. Y. Matsuzaki, and I. Yasuda, *J. Electrochem. Soc.*, **147** (5), 1630 (2000).
16. M. J. Jørgensen and M. Mogensen, *J. Electrochem. Soc.*, **148** (5), A433 (2001).

17. N. T. Hart, N. P. Brandon, M. J. Day, N. Lapeña-Rey, *J. Power Sources*, **106**, 42 (2002).
18. A. C. Müller, D. Herbstritt, E. Ivers-Tiffée, *Solid State Ionics*, **152-153**, 537 (2002).